the first modal frequency and grows rapidly with frequency. The first three modes differ by 8, 24, and 46%, respectively, with the Timoshenko model predicting consistently lower modal frequencies. Beyond the third mode, the models differ qualitatively, with the Timoshenko model having several modes between every mode of the Euler model. For this cross-section, the ratio between the first natural frequency and the Timoshenko shear mode cutoff frequency is only about 15. The transfer function phase, shown in Fig. 2b, reflects even more clearly the difference between the two models. Phase lag of the Timoshenko model grows at a much greater rate than the Euler-Bernoulli beam. This phase behavior is consistent with delay vs frequency dependence obtained using the wave-solution approach (see Fig. 1). The additional phase lag in the Timoshenko model can be attributed to finite delay at high frequencies, and the Euler model predicts delay approaching zero for high frequencies.

For the same hollow cross section, but constructed of T300 composite, the ratio between the first Euler-Bernoulli model modal frequency and the Timoshenko shear mode cutoff frequency is reduced to only 3.2. As shown in Ref. 7, the divergence between the models is even more severe, with the first Euler-Bernoulli modal frequency 55% higher than the first Timoshenko modal frequency. Beyond the first Euler-Bernoulli modal frequency, the Timoshenko model has several modes for each mode of the Euler-Bernoulli model.

V. Validity of Beam Models

As previously demonstrated, the important parameter in determining the range of validity of the beam models is the shear mode cutoff frequency. The Euler-Bernoulli model is accurate only for frequencies much below (by at least a factor of 20) the cutoff frequency. Use of the Euler-Bernoulli model for control sytsem design is justified only if the control bandwidth is much below the cutoff frequency. A design based on the Euler-Bernoulli model that violates that restriction will result in faulty performance predictions because of overestimation of the modal frequencies. Even worse, closed-loop control instability is likely due to underestimation of the phase lag.

Figure 3 provides normalized curves for determining the validity of the Euler-Bernoulli model for various cross sections. It shows the ratio of shear mode cutoff frequency to first natural frequency as a function of normalized length. For the circular cross sections length is normalized by the cross-sectional radius; for the rectangular cross sections length is normalized to the height of the cross section. For example, a control system designed to control the first bending mode of a beam with a circular shell cross section requires that the length-to-cross-sectional ratio be at least 20 to justify the use of the Euler-Bernoulli model.

The Timoshenko beam model is accurate for frequencies well beyond the shear mode cutoff frequency. This fact can be observed by comparing the dispersion curves of the Timoshenko model and the accurate solution.[5] The first branch of the dispersion curve is within 1% of the exact solution. The second branch of the Timoshenko model starts to diverge noticeably from the exact model only at frequencies 20% higher than the cutoff frequency. Few control problems require bandwidths higher than the cutoff frequency. Hence, in most applications Timoshenko beam model is adequate for control modeling.

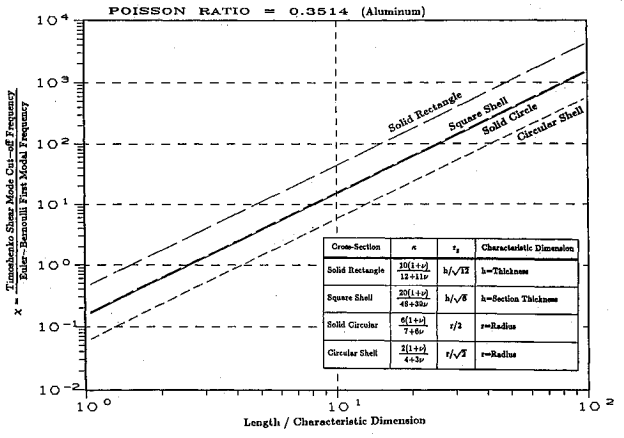

Fig. 3 Normalized curves for determining validity of Euler-Bernoulli beam model.

VI. Conclusions

A study of flexible manipulator link modeling provides quantitative guidelines for determining the range of validity of the frequently used Euler model. Use of the Euler model beyond the range introduces severe errors in the transfer functions required for control analysis. A wave propagation analysis is necessary to interpret the frequency response and calculate the time delay present in a noncollocated control system.

References

[1]Sunada, W. H., and Dubowsky, S., "On the Dynamic Analysis and Behavior of Industrial Robotic Manipulators with Elastric Members," American Society of Mechanical Engineers Paper 82-DET-45, Sept. 1982.

[2]Von Flotow, A. H., "Disturbance Propagation in Structural Networks; Control of Large Space Structures," Ph.D. Thesis, Dept. of Aeronautics and Astronautics, Stanford Univ., Stanford, CA, June 1984.

[3]Wie, B., "On the Modeling and Control of Flexible Space Structures," Guidance and Control Lab., Stanford Univ., Stanford, CA, SUDAAR 525, June 1981.

[4]Cannon, R. H., Jr., and Schmitz, E., "Initial Experiments on the End-Point Position Control of a Flexible One-Link Manipulator," *International Journal of Robotics Research,* Vol. 3, No. 3, Fall 1984, pp. 62–75.

[5]Graff, K. F., *Wave Motion in Elastic Solids,* Ohio State Univ. Press, Columbus, 1975.

[6]Cowper, G. R., "The Shear Coefficient in Timoshenko's Beam Theory," *Journal of Applied Mechanics,* June 1966, pp. 335–340.

[7]Spector, V. A., and Flashner, H., "Flexible Manipulator Modeling in Control System Development," *Proceedings of the AIAA Guidance, Navigation and Control Conference,* AIAA, New York, 1987, pp. 213–220.

Tracking with Paired Angle Measurement Sensors

Thomas R. Blackburn*
McDonnell Douglas Space Systems Company, Huntington Beach, California

Nomenclature

$\boldsymbol{d}$	= target line-of-sight unit direction vector
E	= assumed energy level
$\boldsymbol{H}$	= observation vector sensitivity to state vector change matrix
h	= transformation from the trajectory state to the observation vector
$\boldsymbol{p}_S, \boldsymbol{p}_T$	= sensor and target position vectors, respectively
$\boldsymbol{R}$	= observation vector noise covariance matrix, or the distance from Earth's center, as appropriate

Received May 9, 1988; revision received July 28, 1988.

*Manager, Guidance and Navigation.

r_1, r_2 = ranges from sensor 1 and 2 to the target, respectively
v_S, v_T = sensor and target velocity vectors, respectively
x = target state
Δp = position displacement between the two sensors
ζ = target pseudoelevation angle
θ = target pseudoazimuth angle
Φ = four observation vectors stacked into a single vector
μ = gravitational constant

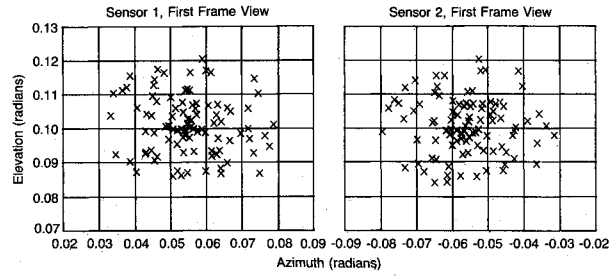

Fig. 1 A threat cloud appears different to two sensors.

Introduction

VIEWS of a hypothetical intercontinental ballistic missile (ICBM) attack as seen by two infrared scanning sensors on their first scan cycle are shown in Fig. 1. The scan is viewed from different angles and, consequently, looks different to the two observers.

The images are detected as they are swept across a column of photodetectors. Consequently, each has an individual observation time dependent on its azimuth. If one knew which image in the sensor 2 field corresponded to an image in the sensor 1 field, the initiation of a target track would be relatively straightforward. This problem generally has been addressed[1] by establishing track files with the individual sensors. If the target objects are known to be in exoatmospheric ballistic trajectories, small differences in acceleration between the target and the observer due to gravity or sensor acccelera-tion make range and range rate weakly observable. If both targets and observers are in ballistic trajectories, this observability is very weak, necessitating the tracking of objects for an extended time with a very precise instrument to establish that a series of observations does indeed correspond to the same unique trajectory. Once track files are established by the individual sensors, the correlation of the redundant files between the sensors is relatively easy. The alternate approach to be described correlates observations between sensors before a track file is established. The track initialization exploits the range information inherent in stereoscopic vision, and provides the range information lacking in the conventional approach.

Approach

A concept previously developed[2] is relied upon here. In this approach a coordinate set is established in which the x axis is along the position difference vector (ΔP) between the two sensors, the z axis is aligned along the average sensor position vector, and the y axis completes the right-hand set. One rotates the y axis to align it with a line of sight, first with an Euler rotation ζ about the x axis and a subsequent θ rotation about the z axis. If this is done by each sensor to the same object, the ζ values for the two sensors will be equal. Sensor-to-sensor correlation thus becomes a process of matching ζ values between sensors. The respective ranges to the target (r_i) can be obtained with θ_1, θ_2, Δp, and the law of sines.

$$r_i = \Delta P \cos\theta_i / \sin(\theta_2 - \theta_1) \tag{1}$$

The three points defined by the target and the two sensors form a plane. If other targets fall in this plane they will have the same ζ angles, and a condition referred to as "ghosting" exists. Lines of sight cross at points other than at real objects and thus form ghost objects. The condition can be detected by observing multiple ζ angles of approximately the same value and deferring the correlation until a later time.

With a method for two-probe correlation defined, the method for establishing and continuing track files will be defined in eight steps.

1) Update existing track files with new data. The inherent feature of recursive least-square estimation algorithms of making a priori predictions of the next expected observation is exploited. The actual observation nearest to this prediction is chosen to update the track file.

2) Compute $\zeta - \theta$ files for the remaining unassigned observations.

3) Pair up observations from the first two frames of data for each sensor separately. This is done by picking the nearest eligible observation on the second frame cycle to the position predicted for an object in the first frame cycle. The prediction is made by adding a line of sight increment to the first frame observation. This increment can be obtained with information extracted from the focal-plane signal processing, from a neighboring object already established in track, or from a priori assumptions about the nature of the trajectory, as appropriate.

4) Interpolate the $\{\zeta\ \theta\ \Delta p\}'$ pairs from the first two-frame cycles to a common time. Because there are only two observations, the interpolation will be linear. This step satisfies the stipulation that observations be made simultaneously in the ζ-matching method previously defined. This can become impractical, however, if the scan cycle time is too long.

5) For a given ζ value in the sensor 1 interpolated file, find its closest equivalent in the sensor 2 file. This search-matching process can be made more efficient by ordering the $\zeta - \theta$ files by increasing values of ζ, and so the search is systematic rather than exhaustive. There are two conditions under which the eight-step procedure is skipped out of here. If there is no $\zeta - 2$ value within a given distance from the $\zeta - 1$ value, it is assumed that the second sensor has not acquired the object yet. If there is more than one $\zeta - 2$ value within another given distance of $\zeta - 1$, the ghosting condition is assumed.

6) Make an initial estimate of the target state (x_0) with the paired vectors of step 4 by computing range with Eq. (1), and target position with

$$p_T = p_S + rd \tag{2}$$

and differentiating,

$$v_T = v_S \dot{r}d + r\dot{d} \tag{3}$$

The $\dot{d}$ is constructed

$$\dot{d} = (d_2 - d_1)/\Delta t \tag{4}$$

and d_2 and d_1 are constructed from the first and second observations, respectively. Either sensor can be used in these equations. Range rate is inferred by assuming the energy level of a typical ICBM.

$$\dot{r} = -q \cdot d - \sqrt{(q \cdot d)^2 - q^2 + 2(E - \mu/R_T)} \tag{5}$$

where

$$q \triangleq V_s + r\dot{d} \tag{6}$$

The algorithm is not particularly sensitive to errors in this energy assumption.

7) Least-square fit four observations to a trajectory. The four observations came first from the pairings of step 2 and the second-level pairing of step 4. Stacking up four two-

dimensional observations into an eight-vector Φ, one can estimate the a priori observation vector

$$\Phi_0 = h(x_0) \tag{7}$$

and form

$$\Delta\Phi = \Phi - \Phi_0 = H\Delta x \tag{8}$$

We use a square-root information filter technique[3] to obtain a least-square solution to this equation. This scheme also provides the computed error residual ϵ, the errors in the fit of the observations to the observations computed from the state estimate x_0. The χ^2 scalar is computed:

$$\chi^2 = \epsilon' R^{-1} \epsilon \tag{9}$$

8) If the χ^2 fit is greater than a specified value, declare one of the chosen frame cycle 2 observations ineligible and return to step 3. This step forms a recursive loop around steps 3-8, which is cycled upon until a satisfactory fit is found or a limit is reached. The limit may be that there are no eligible observations left within a specified search area or that a specific number of cycles has been performed. The algorithm can reject good matches, and so it is necessary to constrain the looping in case it misses the right set. If a χ^2 fit falls below the specified threshold, the state vector is accepted as an initialized track file.

$$x = x_0 + \Delta x \tag{10}$$

An inherent synergism is built into this procedure in that four observations are needed for step 4 to synchronize the observations in time, and four are also needed in step 7 to satisfy the "overconstrained" condition. The overconstrained condition asserts that a trajectory can always be fitted to three or fewer observations, but only a real trajectory can be fitted to four or more correctly correlated observations (ignoring the ghosting problem), and so it is necessary to fit at least four observations to get a good test. The fact that the four observations have been taken from two different vantage points provides complete observability and will, in general, provide good state estimates. This breaks down if the observers are placed too close together; then a geometric dilution of precision condition comes into play.

Conclusions

A new data processing architecture of correlating and tracking objects with paired passive sensors has been developed and verified by Monte Carlo simulation. The simulations show 80% reductions in the average time it takes to establish objects in track and greater than 98% reductions in computing run times in comparison with the established procedure of merging tracks from sensors operating autonomously.

References

[1]"Sensor to Sensor (Probe-to-Probe) Correlation Study," Massachusetts Inst. of Technology, Cambridge, MA, Lincoln Lab. Rept. SDP-245, Sept. 1982.

[2]Blackburn, T. R., "A Practical Correlation Test for Cooperative Passive Optical Sensors," *Journal of Guidance, Control, and Dynamics*, Vol. 6, Jan.-Feb. 1983, p. 62.

[3]Bierman, G. J., *Factorization Methods for Discrete Sequential Estimation*, Academic, New York, 1977, p. 71.